Degree of fourth-order coherence by double Hanbury Brown–Twiss detections*

Zhang Yu-Chi(张玉驰)[a], Li Yuan(李 园)[a)b)], Guo Yan-Qiang(郭龑强)[a)], Li Gang(李 刚)[a)], Wang Jun-Min(王军民)[a)], and Zhang Tian-Cai(张天才)[a)†]

[a)] *State Key Laboratory of Quantum Optics and Quantum Optics Devices, Institute of Opto-Electronics, Shanxi University, Taiyuan* 030006, *China*

[b)] *State Key Laboratory for Superlattices and Microstructures, Institute of Semiconductors, Chinese Academy of Sciences, Beijing* 100083, *China*

(Received 27 October 2009; revised manuscript received 20 January 2010)

Photon quantum statistics of light can be shown by the high-order coherence. The fourth-order coherences of various quantum states including Fock states, coherent states, thermal states and squeezed vacuum states are investigated based on a double Hanbury Brown–Twiss (HBT) scheme. The analytical results are obtained by taking the overall efficiency and background into account.

Keywords: fourth-order coherence, quantum state, single-photon counting
PACC: 4250, 4225K, 0530

1. Introduction

The landmark experiment on photon correlation by Hanbury Brown and Twiss (HBT) in 1956[1] stimulated the birth of modern quantum optics.[2] With the development of modern optics and electronics, the technology of single-photon detection has advanced rapidly in recent years. Commercial high efficiencies single-photon counting modules (SPCMs) and the photon-number-resolving detectors have been widely used for scientific research and sensitive measurement. Due to their high quantum efficiency in the visible and near infrared range, low dark count and fast response they are becoming key tools in quantum optics and quantum information science[3] for single-photon source determination,[4] quantum state preparation,[5,6] quantum logic gates,[7] and so forth.

Higher-order coherence $g^{(n)}$, regarded as an important quantity for revealing the quantum statistics of light, plays a key role in understanding the coherence of quantum states.[8,9] With the development of experimental techniques for fast and sensitive measurements of light, the higher-order interference behaves differently from the lower-order ones.[10] For uncorrelated and distinguishable input photons, the fourth-order interference is readily understood in terms of the particle or wave behaviour of each photon action.[11] For many years, much effort has been made to study the fourth-order interference in parametric down conversion[12−14] and ghost imaging.[15] The fourth-order coherence describes the photon correlation of the light field at four separated points in space and time. Usually, there are four photon detectors needed, and the quantum statistics may be strongly affected by the experimental conditions, such as quantum efficiency and background. Although the on-off SPCMs cannot respond to multi-photons during dead time,[16,17] before high efficiency photon-number-resolving detectors[18] can be developed and commercialized they are currently still an option for determining the statistical properties of the light fields.[19]

In the present paper, the effects of the fourth-order coherence for various quantum states are discussed and compared based on the double HBT schemes formed by four SPCMs. We take into account the overall efficiency and the dark counts of the detection.[20] The measurements of the fourth-order coherence $g^{(4)}$ are obtained. The results show how the higher-order coherences of different quantum states including Fock states, coherent states, thermal states and squeezed vacuum states are essentially affected by experimental conditions.

*Project supported by the National Natural Science Foundation of China (Grant Nos. 10974125, 60821004, 60808006, 60978017 and 60578018), and the State Basic Key Research Program of China (Grant No. 2006CB921102).
†Corresponding author. E-mail: tczhang@sxu.edu.cn
© 2010 Chinese Physical Society and IOP Publishing Ltd

2. Model

We consider the system in Fig. 1 where the traditional single HBT configuration is expanded from two SPCMs to four SPCMs. Assume that the input field $|\psi\rangle$ has an intrinsic photon distribution $P_{\rm in}(n)$. The overall detection efficiency, including the optical collection efficiency, propagation efficiency and quantum efficiency of the photon detectors, is η. This overall efficiency can be regarded as the attenuation (a beam splitter) of the incident field by attenuator B0 with a transmission of $1-\eta$ while the rest of the detection is perfect. For simplicity, we assume that all the SPCMs have the same efficiencies. The background

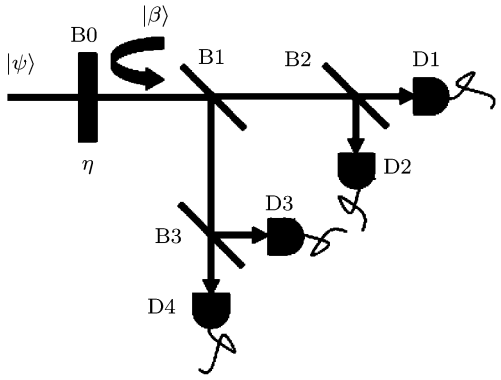


Fig. 1. Double HBT configuration based on four SPCMs with overall efficiency η and background $|\beta\rangle$. B1, B2, B3 are 50/50 lossless beam splitters.

is a random statistical light field with a Poissonian distribution[16] and can be simulated by a weak random field $|\beta\rangle$ which statistics is $P_{\rm in}(n) = \gamma^n \exp(-\gamma)/n!$, where $\gamma = |\beta|^2$. B1, B2, B3 are 50/50 lossless beam splitters.

The photon number distribution after the beam splitter, when the extra vacuum state input from the beam splitter is taken into account, is[21]

$$P_{\rm tr}(m) = \sum_{n=m}^{\infty} P_{\rm in}(n) \frac{n!}{m!\,(n-m)!} \eta^m \,(1-\eta)^{(n-m)}\,. \quad (1)$$

The beam is then mixed at beam splitter B1 with a weak background light, and the photon number distribution can be written as[22]

$$P_{\rm mix}(L) = \sum_{m=0}^{L} \frac{\gamma^{(L-m)}}{(L-m)!} {\rm e}^{-\gamma} P_{\rm tr}(m). \quad (2)$$

Here, L is the number of photons incident on B1. If N photons are transmitted, then L–N photons are reflected and for these N photons arriving at beam splitter B2 there are K photons detected by D1 and N–K photons by D2. On the other hand, of the L–N photons incident on B3, M photons are detected by D3 and $(L$–$N)$–M by D4.

The resulting probability of detecting K, N–K, M and $(L$–$N)$–M photons at D1, D2, D3 and D4, respectively, can be written as $P(K,\ N$–$K,\ M,\ (L$–$N)$–$M)$. Since one SPCM gives only one count during dead time for one or more than one incident photon, there are in total sixteen possible photon probabilities. Since B1, B2, B3 are 50/50 lossless beam splitters and the four SPCMs are identical, there are indeed five different photon probabilities:

$$P(1,1,1,1) = \sum_{L=4}^{\infty} P_{\rm mix}(L) \sum_{N=2}^{L-2} \sum_{K=1}^{N-1} \sum_{M=1}^{(L-N)-1} \left(\frac{1}{2}\right)^{(2L)} \frac{L!}{K!\,(N-K)!M!\,((L-N)-M)!}, \quad (3a)$$

$$P(0,1,1,1) = P(1,0,1,1) = P(1,1,0,1) = P(1,1,1,0)$$
$$= \sum_{L=3}^{\infty} P_{\rm mix}(L) \sum_{N=2}^{L-1} \sum_{K=1}^{N-1} \left(\frac{1}{2}\right)^{(2L)} \frac{L!}{K!\,(N-K)!\,(L-N)!}, \quad (3b)$$

$$P(1,0,0,1) = P(1,1,0,0) = P(0,0,1,1) = P(0,1,1,0) = P(1,0,0,1) = P(0,1,0,1)$$
$$= \sum_{L=2}^{\infty} P_{\rm mix}(L) \sum_{N=1}^{L-1} \left(\frac{1}{2}\right)^{(2L)} \frac{L!}{N!\,(L-N)!}, \quad (3c)$$

$$P(0,1,0,0) = P(0,0,1,0) = P(0,0,0,1) = P(1,0,0,0) = \sum_{L=1}^{\infty} P_{\rm mix}(L) \left(\frac{1}{2}\right)^{2L}, \quad (3d)$$

$$P(0,0,0,0) = P_{\rm mix}(0). \quad (3e)$$

For a single-mode field, $g^{(4)}$ is independent of delay time τ and the fourth-order coherence can be expressed as

$$g^{(4)}=\frac{\langle n_1n_2n_3n_4\rangle}{\langle n_1\rangle\langle n_2\rangle\langle n_3\rangle\langle n_4\rangle}=\frac{\langle n_1n_2n_3n_4\rangle}{\left[\frac{1}{4}\langle n\rangle\right]^4}=\frac{\sum\limits_{n_1n_2n_3n_4}(n_1n_2n_3n_4)\,P(n_1,n_2,n_3,n_4)}{\left[\frac{1}{4}\sum\limits_n nP(n)\right]^4}=\frac{P(1,1,1,1)}{\left[\frac{1}{4}\langle n\rangle\right]^4}, \quad (4)$$

where $\langle n\rangle$ is the mean photon number which is defined as

$$\begin{aligned}\langle n\rangle&=\sum_{n=0}^{\infty}nP(n)\\&=4P(1,1,1,1)+3\left[P(1,1,1,0)+P(1,1,0,1)+P(1,0,1,1)+P(0,1,1,1)\right]\\&\quad+2\left[P(1,1,0,0)+P(0,0,1,1)+P(1,0,1,0)+P(1,0,0,1)+P(0,1,1,0)+P(0,1,0,1)\right]\\&\quad+\left[P(1,0,0,0)+P(1,0,0,0)+P(0,0,1,0)+P(0,0,0,1)\right]+0P(0,0,0,0)\\&=4P_4+3P_3+2P_2+P_1+0P_0, \quad (5)\end{aligned}$$

where P_0, P_1, P_2, P_3 and P_4 denote the probabilities of detecting simultaneously 0, 1, 2, 3 and 4 photons by the four SPCMs, respectively. $P(n_1,\ n_2,\ n_3,\ n_4)$ is the resulting probability of detecting n_1 photons on detector 1, n_2 photons on detector 2, and so on simultaneously. For SPCM which gives only one count during dead time for greater than or equal one incident photon, $g^{(4)}$ can be written as Eq. (4).

3. Discussion for various input states

3.1. Coherent state

For incident coherent field $|\alpha\rangle$, the photon distribution is a well-known Poissonian distribution, i.e.

$$P_{\rm in,C}(n)=\frac{\alpha^n{\rm e}^{-\alpha}}{n!}, \quad (6)$$

where α is the mean photon number. For a given overall detection efficiency η and background $|\beta\rangle$, from Eqs. (1)–(3) we can obtain the photon detection probabilities and mean photon number as follows:

$$P_{4\rm C}={\rm e}^{-\gamma-\alpha\eta}\left[{\rm e}^{(\gamma+\alpha\eta)/4}-1\right]^4, \quad (7a)$$

$$P_{3\rm C}=4{\rm e}^{-\gamma-\alpha\eta}\left[{\rm e}^{(\gamma+\alpha\eta)/4}-1\right]^3, \quad (7b)$$

$$P_{2\rm C}=6{\rm e}^{-\gamma-\alpha\eta}\left[{\rm e}^{(\gamma+\alpha\eta)/4}-1\right]^2, \quad (7c)$$

$$P_{1\rm C}=4{\rm e}^{-\gamma-\alpha\eta}\left[{\rm e}^{(\gamma+\alpha\eta)/4}-1\right], \quad (7d)$$

$$P_{0\rm C}={\rm e}^{-\gamma-\alpha\eta}, \quad (7e)$$

$$\langle n\rangle_{\rm C}=4-4{\rm e}^{-(\gamma+\alpha\eta)/4}. \quad (7f)$$

The fourth-order coherence $g_{\rm C}^{(4)}$ is given as

$$g_{\rm C}^{(4)}=1. \quad (8)$$

This result indicates that the fourth-order coherence for coherent state is not affected by the overall efficiency and background.

3.2. Fock states

Fock state is a valuable quantum resource for ultra-high sensitive measurement[23] or quantum information[3] and there are many proposals to generate Fock states with a large number of photons.[24–26] In fact, the measurement of Fock state is also a challenge. If the input field is Fock state $|n\rangle$, we have $P_{\rm in,F}(n)=1$. That means that one can find only n photons in Fock state $|n\rangle$. When the total detection efficiency and the background are taken into account, the photon number distribution can be written as

$$P_{\rm mix,F}(L)=\sum_{m=0}^{L}\frac{\gamma^{(L-m)}n!}{(L-m)!m!(n-m)!}\times{\rm e}^{-\gamma}\eta^m(1-\eta)^{n-m}. \quad (9)$$

Particularly, for the single-photon state the photon number distribution is

$$P_{\rm mix,F}(L)|_{n=1}=\frac{\gamma^L}{L!}{\rm e}^{-\gamma}(1-\eta)+\frac{\gamma^{(L-1)}}{(L-1)!}{\rm e}^{-\gamma}\eta. \quad (10)$$

By using Eqs. (3) and (10) we can find the measured probabilities of photon number of a single photon state to be

$$P_{4\rm F}|_{n=1}={\rm e}^{-\gamma}\left({\rm e}^{\gamma/4}-1\right)^3\left({\rm e}^{\gamma/4}-1+\eta\right),$$

$$P_{3\rm F}|_{n=1}=-{\rm e}^{-\gamma}\left({\rm e}^{\gamma/4}-1\right)^2\left[4+{\rm e}^{\gamma/4}(\eta-4)-4\eta\right],$$

$$P_{2\rm F}|_{n=1}=-3{\rm e}^{-\gamma}\left({\rm e}^{\gamma/4}-1\right)\left[2+{\rm e}^{\gamma/4}(\eta-2)-2\eta\right],$$

$$P_{1\rm F}|_{n=1}={\rm e}^{-\gamma}\left[{\rm e}^{\gamma/4}(4-3\eta)+4(\eta-1)\right],$$

$$P_{0\rm F}|_{n=1}={\rm e}^{-\gamma}(1-\eta),$$

$$\langle n\rangle_{\rm F}|_{n=1} = 4 + \eta {\rm e}^{-\gamma/4} - 4{\rm e}^{-\gamma/4}. \quad (11)$$

Apparently, the fourth-order coherence $g_{\rm F}^{(4)}$ in the single-photon state is then given by

$$g_{\rm F}^{(4)}\Big|_{n=1} = \frac{256\left({\rm e}^{\gamma/4}-1\right)^3\left(4{\rm e}^{\gamma/4}-4+\eta\right)}{\left(4{\rm e}^{\gamma/4}-4+\eta\right)^4}. \quad (12)$$

In the case of no background, i.e. $\gamma = 0$, we obtain $g_{\rm F}^{(4)}|_{n=1} = 0$. This shows that $g_{\rm F}^{(4)}$ of the single-photon state can be perfectly determined since the single-photon state exhibits anti-bunching effect.

It is important to know how the background and the efficiency affect the Fock state measurement. Figure 2 shows curves for $g_{\rm F}^{(4)}$ (n=1, 2, 3, 4 corresponding to Figs. 2(a)–2(d), respectively) versus detection efficiency for different backgrounds. The solid lines correspond to the small-number Fock states without any background. The dash, dot and dash–dot lines correspond to backgrounds of $\gamma = 0.001$, 0.01 and 0.1, respectively. For a given detection efficiency, the existence of a background gives higher value of $g_{\rm F}^{(4)}$, but this effect can be washed out as photon number n increases. Without the background all measurements can approach to the outmost limits, which are determined by the on–off detection of the SPCMs, as the detection efficiency goes to unit. For a given background, the results firstly decrease and then increase as the total detection efficiency approaches to unit. This can be well understood. The random Poissonian statistics of the background will dominate the final results in the case of a weak and fragile quantum state when the detection efficiency is small. As the detection efficiency is higher, the Fock state itself dominates the system which results in the decrease of $g_{\rm F}^{(4)}$. But if the overall efficiency is better, which means more multi-photons are missing the result of higher value of $g_{\rm F}^{(4)}$ is apparent. Consequently, the eventual measurement is determined by all these factors. This is why in general there exists overall efficiency η, at which $g_{\rm F}^{(4)}$ is minimum (see Fig. 2).

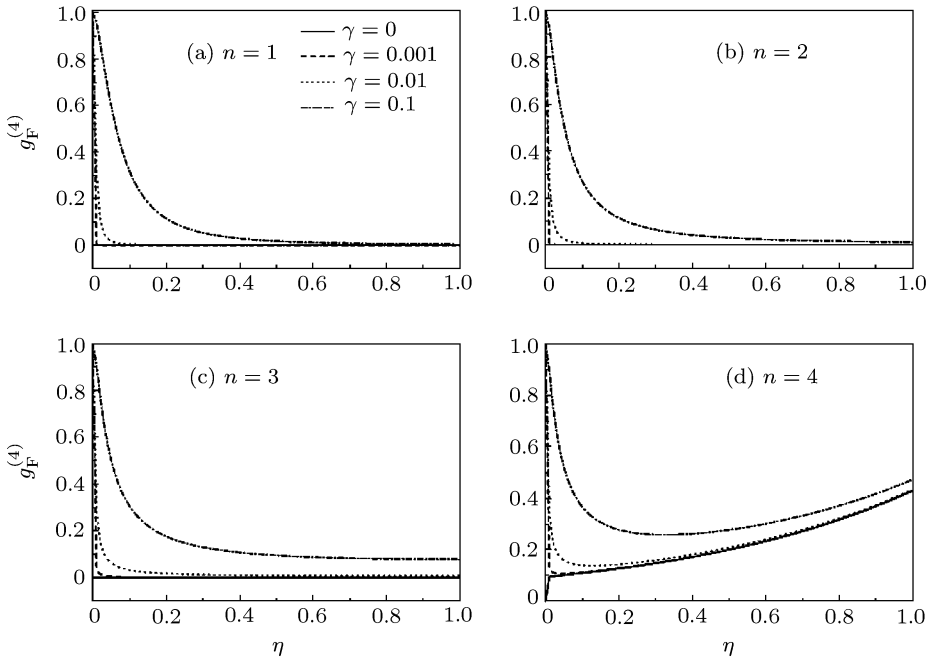


Fig. 2. Curves for the fourth-order coherence $g_{\rm F}^{(4)}$ of Fock states (n = 1, 2, 3, 4 corresponding to subfigures (a), (b), (c), (d), respectively) versus detection efficiency for different backgrounds.

3.3. Thermal field

A single-mode thermal field satisfies the Bose–Einstein distribution

$$P_{\rm in,T}(n) = \frac{(\alpha)^n}{(1+\alpha)^{n+1}}, \quad (13)$$

where $\alpha = [\exp(\hbar\omega/k_{\rm B}T) - 1]^{-1}$ is the mean photon number. The thermal field is a typical incoherent source which shows the bunching effect and a super-Poissonian photon distribution. From Eqs. (1), (2) and (13), the probability $P_{\rm mix,T}(L)$ of detecting L photons at beam splitter B1 for the single-mode thermal field is

$$P_{\rm mix,T}(L) = \sum_{m=0}^{L} \frac{\gamma^{(L-m)}}{(L-m)!} {\rm e}^{-\gamma} \frac{(\eta\alpha)^m}{(1+\eta\alpha)^{m+1}}. \tag{14}$$

Using Eqs. (3) and (14), we arrive at

$$P_{4\rm T} = 1 - \frac{16}{4+3\eta\alpha}{\rm e}^{-3\gamma/4} - \frac{16}{4+\eta\alpha}{\rm e}^{-\gamma/4} + \frac{12}{2+\eta\alpha}{\rm e}^{-\gamma/2} + \frac{1}{1+\eta\alpha}{\rm e}^{-\gamma}, \tag{15a}$$

$$P_{3\rm T} = \frac{48}{4+3\eta\alpha}{\rm e}^{-3\gamma/4} + \frac{16}{4+\eta\alpha}{\rm e}^{-\gamma/4} - \frac{24}{2+\eta\alpha}{\rm e}^{-\gamma/2} - \frac{4}{1+\eta\alpha}{\rm e}^{-\gamma}, \tag{15b}$$

$$P_{2\rm T} = \frac{12}{2+\eta\alpha}{\rm e}^{-\gamma/2} - \frac{48}{4+3\eta\alpha}{\rm e}^{-3\gamma/4} + \frac{6}{1+\eta\alpha}{\rm e}^{-\gamma}, \tag{15c}$$

$$P_{1\rm T} = \frac{16}{4+3\eta\alpha}{\rm e}^{-3\gamma/4} - \frac{4}{1+\eta\alpha}{\rm e}^{-\gamma}, \tag{15d}$$

$$P_{0\rm T} = \frac{{\rm e}^{-\gamma}}{1+\eta\alpha}, \tag{15e}$$

$$\langle n\rangle_{\rm T} = 4 - 16\frac{{\rm e}^{-\gamma/4}}{4+\eta\alpha}. \tag{15f}$$

Similarly, we obtain

$$g_{\rm T}^{(4)} = \frac{256\left(1 + \dfrac{{\rm e}^{-\gamma}}{1+\alpha\eta} + \dfrac{12{\rm e}^{-\gamma/2}}{2+\alpha\eta} - \dfrac{16{\rm e}^{-\gamma/4}}{4+\alpha\eta} - \dfrac{16{\rm e}^{-3\gamma/4}}{4+3\alpha\eta}\right)}{\left(4 - \dfrac{16{\rm e}^{-\gamma/4}}{4+\alpha\eta}\right)^4}. \tag{16}$$

In the case of no background and nonzero detection efficiency, we have

$$g_{\rm T}^{(4)} = \frac{1 + \dfrac{1}{1+\alpha\eta} + \dfrac{12}{2+\alpha\eta} - \dfrac{16}{4+\alpha\eta} - \dfrac{16}{4+3\alpha\eta}}{\left(1 - \dfrac{4}{4+\alpha\eta}\right)^4}. \tag{17}$$

Figure 3(a) shows the results based on Eqs. (16) and (17) with $\alpha = 1$. The solid, dash, dot and dash–dot lines correspond to backgrounds with $\gamma = 0$, 0.001, 0.01, and 0.1, respectively.

Figure 3(b) shows the results of the measured fourth-order coherence $g_{\rm T}^{(4)}$ in thermal field versus mean photon number for different total detection efficiencies and backgrounds. The solid lines are for the results without background and with detection efficiency being 1, while the dash lines are for a background of 0.001 and an efficiency of 0.05.

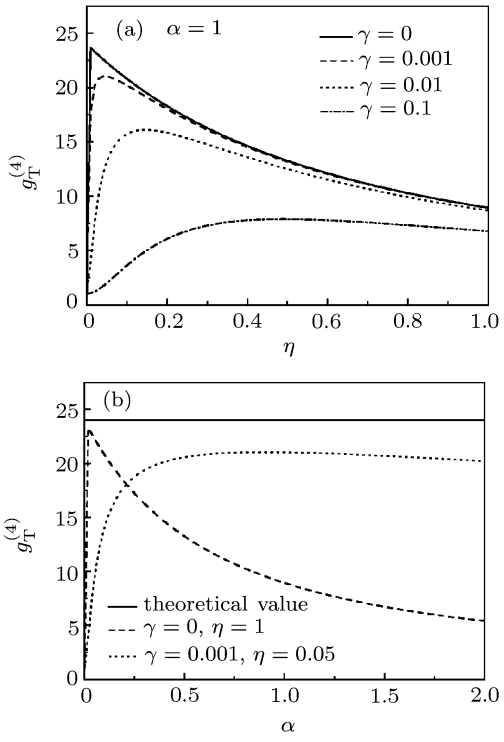


Fig. 3. Curves for the fourth-order coherence $g_{\rm T}^{(4)}$ in thermal field versus detection efficiency ($\alpha = 1$) (a) and mean photon number (b) for different backgrounds.

3.4. Squeezed vacuum state

The squeezed vacuum state (SVS) is a very important quantum-light state in quantum information processing with continuous variables and entanglement generation. A single-mode SVS can be written as $|\xi\rangle = \hat{S}(\xi)|0\rangle$. Here the squeezing operator is $\hat{S}(\xi) = \exp\left(\xi^* \hat{a}^2/2 - \xi \hat{a}^{\dagger 2}/2\right)$, where $\xi = r\exp(\mathrm{i}\theta)$, with $r = |\xi|$ being the squeezing parameter. The photon number distribution can be expressed as

$$P_{\mathrm{in,SVS}}(2n) = \frac{(\tanh r)^{2n}(2n)!}{\cosh r\,(n!2^n)^2}. \tag{18}$$

The mean photon number, and the fourth-order coherence for an ideal SVS can be expressed respectively as

$$\langle n_{\mathrm{sq}}\rangle = \sinh^2 r, \tag{19a}$$

$$g^{(4)}_{\mathrm{SVS}} = \frac{\cosh^4 r}{\sinh^4 r}. \tag{19b}$$

According to Eqs. (1)–(5) and (18), we can similarly obtain the fourth-order coherence $g^{(4)}_{\mathrm{SVS}}$ of SVS based on the double HBT configuration. Here for clarity, we have omitted the complex and tedious expressions but show the numerical results. Figure 4(a) shows the fourth-order coherence $g^{(4)}_{\mathrm{SVS}}$ in SVS based on the double HBT configuration as functions of the detection efficiency and squeezing parameter ($r = 1$) for various backgrounds. The changes in photon statistics are similar to those of a thermal field (see Fig. 3(a)), but the range of change of the parameters are larger due to the well-known super-bunching effect of the SVS.

Figure 4(b) presents $g^{(4)}_{\mathrm{SVS}}$ as a function of the squeezing parameter r. The solid lines are for the ideal values and the dash lines are for zero background and perfect efficiency. The dot lines correspond to 0.001 for the background and 5% for the efficiency, which basically corresponds to the usual experimental conditions. When the squeezing increases, the $g^{(4)}_{\mathrm{SVS}}$ approaches its true photon statistics and is no longer sensitive to the background and the overall efficiency. The reason is that the bunching effect of an SVS becomes weak as squeezing increases.[26]

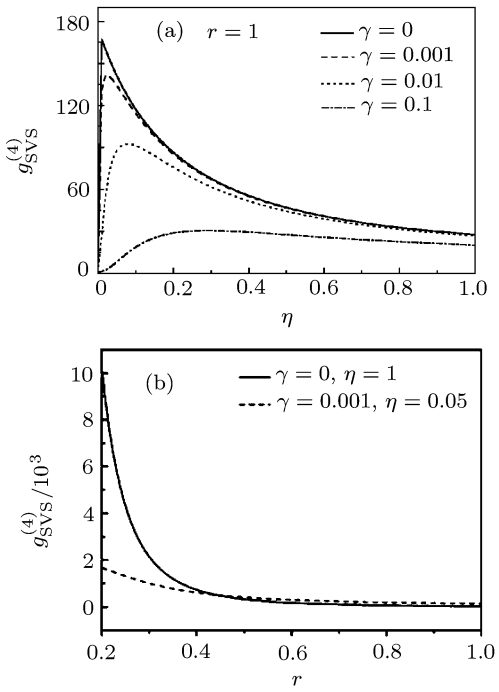


Fig. 4. Curves for the fourth-order coherence $g^{(4)}_{\mathrm{SVS}}$ in a squeezed vacuum state versus detection efficiency ($r = 1$) (a) and the squeezing parameter (b) for different backgrounds.

4. Conclusion

We discussed the higher-order photon statistical properties for several states, from classical to quantum states, based on the double HBT scheme consisting of four on–off SPCMs. The fourth-order coherence $g^{(4)}$ is calculated by taking the overall efficiency and the background into account. The results show that the fourth-order coherence can be detected approximately by this double HBT system, but for different input states, including Fock states, coherent states, thermal states and squeezed vacuum states, the measured results are quite affected by the experimental conditions. The multiple single photon detectors can be used to detect effectively the multi-photon events. The whole analysis is based on the practical experimental conditions and the results can help us understand the capabilities of single-photon counters, which can essentially reveal the real photon statistics of various quantum states. In connection with non-Gaussian measurement, the homodyne detection[27] and post-selection processing, the results and the treatment provided here may be extended to quantum state preparation[5] and remote quantum cloning.[7]

References

[1] Hanbury-Brown R and Twiss R Q 1956 *Nature* **178** 1046

[2] Glauber R J 1965 *Quantum Optics and Electronics* (New York: Gordon and Breach) p. 63

[3] Knill E, Laflamme R and Milburn G J 2001 *Nature* **409** 46

[4] McKeever J, Boca A, Boozer A D, Buck J R and Kimble H J 2003 *Nature* **425** 268

[5] Ourjoumtsev A, Brouri R T, Laurat J and Grangier P 2006 *Science* **312** 83

[6] Wakui K, Takahashi H, Furusawa A and Sasaki M 2007 *Opt. Express* **15** 3568

[7] Lu C Y, Zhou X Q, Guhne O, Gao W B, Zhang J, Yuan Z S, Goebel A, Yang T and Pan J W 2007 *Nature Phys.* **3** 91

[8] Glauber R J 1963 *Phys. Rev.* **130** 2529

[9] Titulaer U M and Glauber R J 1965 *Phys. Rev.* **140** B676

[10] Zhang J X, He L X, Zhang T C, Xie C D and Peng K C 1999 *Acta Phys. Sin.* **48** 1230 (in Chinese)

[11] Campos, Richard A, Saleh, Bahaa E A, Teich and Malvin C 1990 *Phys. Rev.* A **42** 4127

[12] Rarity J G and Tapster P R 1989 *J. Opt. Soc. Am.* B **6** 1221

[13] Ou Z Y and Mandel L 1988 *Phys. Rev. Lett.* **61** 50

[14] Wang R P and Zhang H R 2008 *Chin. Phys.* B **17** 194

[15] Liu Q, Chen X H, Luo K H, Wu W and Wu L A 2009 *Phys. Rev.* A **79** 053844

[16] Li G, Zhang T C, Li Y and Wang J M 2005 *Phys. Rev.* A **71** 023807

[17] Li Y, Li G, Zhang Y C, Wang X Y, Wang J M and Zhang T C 2006 *Acta Phys. Sin.* **56** 5779 (in Chinese)

[18] Rosenberg D, Lita A E, Miller A J and Nam S W 2005 *Phys. Rev.* A **71** 061803(R)

[19] Li Y, Zhang Y C, Zhang P F, Guo Y Q, Li G, Wang J M and Zhang T C 2009 *Chin. Phys. Lett.* **26** 074205

[20] Li Y, Li G, Zhang Y C, Wang X Y, Zhang J, Wang J M and Zhang T C 2007 *Phys. Rev.* A **76** 013829

[21] Mandel L and Wolf E 1995 *Optical Coherence and Quantum Optics* (Cambridge: Cambridge University Press) p. 623

[22] Abate J A, Kimble H J and Mandel L 1976 *Phys. Rev.* A **14** 788

[23] Wildfeuer C F, Pearlman A J, Chen J, Fan J Y, Migdall A and Dowling J P 2009 *Phys. Rev.* A **80** 043822

[24] Brown K R, Dani K M, Stamper-Kurn D M and Whaley K B 2003 *Phys. Rev.* A **67** 043818

[25] Varcoe B T H, Brattke S and Walther H 2004 *New J. Phys.* **6** 97

[26] Mahran M H and Satyanarayana M V 1986 *Phys. Rev.* A **34** 640

[27] Zhang T C, Zhang J X, Xie C D and Pend K C 1998 *Acta Phys. Sin.* (Overseas Edition) **7** 340